LiGe(SiMe$_3$)$_3$: A New Substituent for the Synthesis of Metalloid Tin Clusters from Metastable Sn(I) Halide Solutions

Mareike Binder [1], Claudio Schrenk [1], Theresa Block [2], Rainer Pöttgen [2] and Andreas Schnepf [1,*]

[1] Institut für Anorganische Chemie, Universität Tübingen, Auf der Morgenstelle 18, D-72076 Tübingen, Germany; mareike.binder@uni-tuebingen.de (M.B.); claudio.schrenk@uni-tuebingen.de (C.S.)

[2] Institut für Anorganische und Analytische Chemie, Universität Münster, Corrensstrasse 30, D-48149 Münster, Germany; t_bloc02@uni-muenster.de (T.B.); pottgen@uni-muenster.de (R.P.)

[*] Correspondence: andreas.schnepf@uni-tuebingen.de; Tel.: +49-7071-29-76635

check for
updates

Abstract: The most fruitful synthetic route to metalloid tin clusters applies the disproportionation reaction of metastable Sn(I) halide solutions, whereby Si(SiMe$_3$)$_3$ is mostly used as the stabilizing substituent. Here, we describe the synthesis and application of the slightly modified substituent Ge(SiMe$_3$)$_3$, which can be used for the synthesis of metalloid tin clusters to give the neutral cluster Sn$_{10}$[Ge(SiMe$_3$)$_3$]$_6$ as well as the charged clusters {Sn$_{10}$[Ge(SiMe$_3$)$_3$]$_5$}$^-$ and {Sn$_{10}$[Ge(SiMe$_3$)$_3$]$_4$}$^{2-}$. The obtained metalloid clusters are structurally similar to their Si(SiMe$_3$)$_3$ derivatives. However, differences with respect to the stability in solution are observed. Additionally, a different electronic situation for the tin atoms is realized as shown by ^{119m}Sn Mössbauer spectroscopy, giving further insight into the different kinds of tin atoms within the metalloid cluster {Sn$_{10}$[Ge(SiMe$_3$)$_3$]$_4$}$^{2-}$. The synthesis of diverse derivatives gives the opportunity to check the influence of the substituent for further investigations of metalloid tin cluster compounds.

Keywords: co-condensation; disproportionation; germanium; tin; Mössbauer spectroscopy; bulky substituents; metalloid clusters; nanoscaled clusters

1. Introduction

In the last couple of years, the developments in nanotechnology as well as their industrial applications have generated interest in nanoscaled molecular materials [1]. One example of such nanoscaled compounds is the group of metalloid clusters of the general formula M$_n$R$_m$ (n > m; M = Al, Ga, Sn, Pb, Au, etc.; R = N(SiMe$_3$)$_2$, Si(SiMe$_3$)$_3$, etc.) [2]. As the average oxidation state of the metal atoms within such metalloid clusters is between zero and one, these clusters are localized on the border between molecules and the solid state of metals. Consequently, beside a technological interest, also fundamental questions might be addressed by such metalloid cluster compounds [3–5].

In the case of metalloid cluster compounds of tin, we introduced a special synthetic route, applying the disproportionation reaction of a metastable Sn^I halide solution [6,7]. The metastable solution is obtained via a preparative co-condensation technique. Thereby, a Sn^I halide is condensed together with a mixture of an organic solvent and a donor component such as PnBu$_3$ at −196 °C. This leads to a solid matrix, where the monohalides are completely separated from each other by the solvent molecules. After heating the solid matrix to −78 °C, a metastable solution of Sn^I halides is obtained, if the right solvent–donor mixture is used during the co-condensation. Starting from these metastable solutions, we were able to establish a synthetic route to metalloid tin clusters in recent years, whereby it is important to find a suitable substituent which stabilizes the metastable clusters.

The last years have shown that in particular, the bulky $Si(SiMe_3)_3$ [Hyp] substituent is very useful to trap tin-rich metalloid clusters before complete disproportionation to elemental tin occurs. In this way, a variety of clusters with nine or ten tin atoms in the cluster core could be obtained [8–14], for example, $[Sn_9(Hyp)_2]^{2-}$ [15], $[Sn_9(Hyp)_3]^-$ [16], $[Sn_{10}(Hyp)_4]^{2-}$ [17], $[Sn_{10}(Hyp)_5]^-$ [18], and $Sn_{10}(Hyp)_6$ [19]. Especially $[Sn_9(Hyp)_2]^{2-}$, $[Sn_9(Hyp)_3]^-$, and $[Sn_{10}(Hyp)_4]^{2-}$ are of particular interest, since these clusters exhibit an open ligand shell in which the tin atoms are incompletely shielded by the bulky Hyp ligands and can be attacked by Lewis acids. For example, recent investigations with the metalloid tin cluster $[Sn_{10}(Hyp)_4]^{2-}$ have shown that the reaction with $(Ph_3P)Au-S(Hyp)$ [20] undergoes a complicated scrambling of the metal atoms, which results in the intermetalloid cluster $[Au_3Sn_{18}(Hyp)_8]^-$. This cluster is the longest intermetalloid chain compound of tin found to date [21]. Furthermore, $[Sn_{10}(Hyp)_3]^-$ is formed during the reaction of $[Sn_{10}(Hyp)_4]^{2-}$ with $ZnCl_2$ by the elimination of $ZnCl(Hyp)$ [22].

While the syntheses with the Hyp substituent work relatively well, and the resulting clusters are also useful for further investigations, we wondered if a change to a similar substituent might lead to new metalloid clusters with a similar or different size and structure. Herein, we present the first results applying the germanide $[Ge(SiMe_3)_3]^-$ as a substituent during the synthesis of metalloid tin clusters via the disproportionation reaction of Sn^I halides.

2. Results and Discussion

The germanide $[Ge(SiMe_3)_3]^-$ is synthesized by a similar synthetic route to that of the (Hyp) substituent [23]. Hence, first of all, Me_3SiCl and $GeCl_4$ are coupled in the presence of lithium to give $Ge(SiMe_3)_4$ in 72% yield. Afterwards, the germane $Ge(SiMe_3)_4$ is reacted with methyllithium in THF at room temperature for several days, to give the anticipated compound $LiGe(SiMe_3)_3 \cdot 2.75$ THF in 81% yield after recrystallization.

2.1. $Sn_{10}(Ge(SiMe_3)_3)_6$ **1**

After the successful synthesis of $LiGe(SiMe_3)_3$, it was necessary to check if $LiGe(SiMe_3)_3$ can be used for the synthesis of metalloid tin clusters via the disproportionation reaction of a metastable Sn(I) halide solution. For this purpose, we reacted a −78 °C cold Sn^ICl solution (0.2 M) with $LiGe(SiMe_3)_3 \cdot 2.75$ THF. The reaction mixture is slowly warmed to room temperature to give a black-colored reaction solution without any elemental tin precipitates, indicating that the anticipated trapping of intermediates on the way to elemental tin was successful. After some work-up procedures, black crystals of $Sn_{10}[Ge(SiMe_3)_3]_6$ **1** could be obtained at −30 °C from a pentane solution. The molecular structure of **1** is presented in Figure 1, showing that **1** is a metalloid Sn cluster in which the ten tin atoms are arranged in the form of a centaur polyhedron, whereby six $Ge(SiMe_3)_3$ substituents are bound to the cluster core. **1** is thus isostructural to $Sn_{10}(Hyp)_6$, indicating that the substitution of $Si(SiMe_3)_3$ by $Ge(SiMe_3)_3$ does not lead to a different arrangement of the tin atoms in the cluster and that in both cases, the cluster core is completely shielded by the six substituents.

This result directly shows that the $Ge(SiMe_3)_3$ substituent can be used for the synthesis of metalloid tin clusters. Furthermore, **1** is soluble in common organic solvents, such as toluene, THF, and so forth, which is due to its almost completely shielded tin core giving a nearly perfect nonpolar sphere.

As shown in Table 1, the bond distances within **1** fit very well to the bond distances of the already described $Sn_{10}(Hyp)_6$. This shows that also within **1**, two different types of tin atoms are present inside the metalloid cluster, where the average tin–tin distance in the cubic part of the centaur polyhedron (291 pm) fits to the tin–tin distance found in α-tin (281 pm), while the average tin–tin distance in the icosahedral part of the centaur polyhedron (305 pm) is comparable to the average tin–tin distance found in β-tin (307 pm).

The similar tin–tin distances in **1** and $Sn_{10}(Hyp)_6$ show that the larger $Ge(SiMe_3)_3$ substituent has a similar bulkiness to the smaller Hyp substituent. This might be due to the fact that although $Ge(SiMe_3)_3$ is larger than Hyp, it is also bound farther away from the cluster core due to the longer average Ge–Sn

distance of 267.3 pm in **1** with respect to the average Si–Sn distance of 264.2 pm in $Sn_{10}(Hyp)_6$, and both effects compensate each other. However, besides this steric similarity, an electronic difference might be present due to the different electronegativities of Si and Ge.
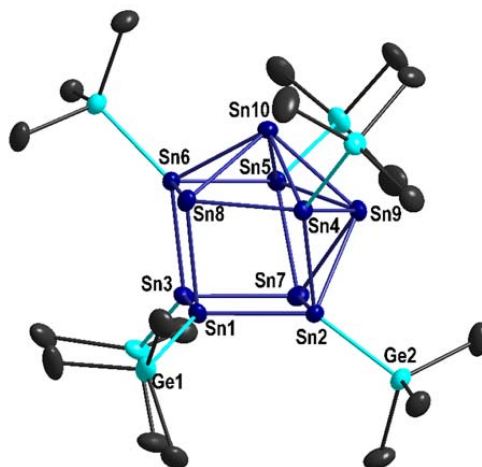

Figure 1. Molecular structure of $Sn_{10}[Ge(SiMe_3)_3]_6$ **1**, without CH_3 groups for clarity (displacement ellipsoids with 50% probability). Selected bond lengths [pm] and angles [°]: Sn1-Sn2: 292.16(3); Sn1-Sn3: 284.85(3); Sn1-Sn8: 288.51(3); Sn2-Sn4: 295.48(3); Sn2-Sn7: 301.94(3); Sn2-Sn9: 304.13(3); Sn3-Sn6: 291.25(3); Sn3-Sn7: 287.32(4); Sn4-Sn8: 292.88(3); Sn4-Sn9: 300.76(3); Sn4-Sn10: 298.77(3); Sn5-Sn6: 294.52(3); Sn5-Sn7: 293.02(3); Sn5-Sn9: 298.53(3); Sn5-Sn10: 301.42(3); Sn6-Sn8: 302.72(3); Sn6-Sn10: 303.42(3); Sn7-Sn9: 310.80(3); Sn8-Sn10: 311.68(3); Sn9-Sn10: 307.29(3); Sn1-Ge1: 266.17(4); Sn2-Ge2: 268.99(4); Sn1-Sn2-Sn7: 89.455(9); Sn2-Sn1-Sn3: 89.500(9); Sn2-Sn1-Sn8: 97.195(10); Sn1-Sn2-Sn4: 80.733(9); Sn2-Sn4-Sn10: 106.176(9); Sn8-Sn4-Sn9: 108.278(10); Ge1-Sn1-Sn8: 108.249(14); Ge2-Sn2-Sn7: 105.781(12).

Table 1. Comparison of selected bond distances [pm] of the metalloid clusters $Sn_{10}[Ge(SiMe_3)_3]_6$ **1** and $Sn_{10}[Si(SiMe_3)_3]_6$.

	$Sn_{10}[Ge(SiMe_3)_3]_6$ **1**	$Sn_{10}[Si(SiMe_3)_3]_6$
Sn1-Sn2	292.2	289.6
Sn1-Sn8	288.5	288.1
Sn2-Sn4	295.5	293.5
Sn3-Sn6	291.3	290.9
Sn4–Sn9	300.8	302.1
Sn5-Sn7	293.0	292.5
Sn5-Sn10	301.4	303.2
Sn7-Sn9	310.8	312.9
Sn1-Ge1	266.2	Sn1–Si1: 264.0

To get a first insight into the electronic situation of **1**, we performed quantum chemical calculations [24–33], whereby similar shared electron numbers (SENs) [34] are calculated for **1** as already obtained for $Sn_{10}(Hyp)_6$, showing that a similar bonding is present inside the cluster. However, the calculated charges of the tin atoms within **1** are very similar, only ranging from +0.12 to −0.11. In the case of $Sn_{10}(Hyp)_6$, the calculated charges show a larger deviation, ranging from −0.51 to +0.25. Hence, by changing the ligand from $Si(SiMe_3)_3$ to $Ge(SiMe_3)_3$, the tin atoms inside $Sn_{10}R_6$ become electronically more similar. This finding is supported experimentally by results of Mössbauer spectroscopy; that is, the ^{119m}Sn Mössbauer spectrum of **1** (Figure 2) shows two quadrupole-split signals A1 and A2 at isomer shifts of $\delta = 2.45(2)$ (with $\Delta E_Q = 1.59(5)$ mm s^{-1} and $\Gamma = 1.05(4)$ mm s^{-1}) and $\delta = 2.51(2)$ (with $\Delta E_Q = 0.54(5)$ mm s^{-1} and $\Gamma = 0.79(4)$ mm s^{-1}) in a fixed area ratio of 60:40 (fitting parameters are given in Table 2). It needs to be said that the area was fixed to avoid correlation

of the quadrupole splitting and the experimental line width; even without fixing, approximately identical results could be received. These two signals of **1** might be assigned to the ligand bound and the naked tin atoms where a ratio of 6:4 is present. Another possibility whereby to describe a 6:4 ratio is realized by dividing the tin atoms in the cluster in those localized in the cubic part and those localized in the icosahedral part of the centaur polyhedron.
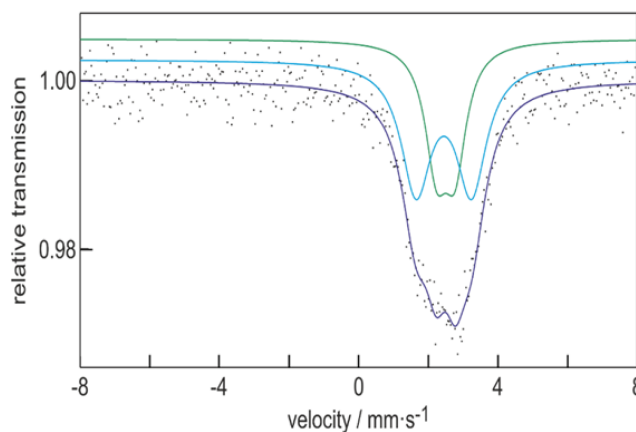

Figure 2. Experimental (data points) and simulated (continuous lines) ^{119m}Sn Mössbauer spectrum of $Sn_{10}[Ge(SiMe_3)_3]_6$ **1** at 5 K. For the fitting parameters, see Table 2.

Table 2. Fitting parameters of the ^{119m}Sn Mössbauer spectroscopic measurement at 5 K. δ = isomer shift, ΔE_Q = electric quadrupole splitting, Γ = experimental line width.

Compound	δ (mm·s^{-1})	ΔE_Q (mm·s^{-1})	Γ (mm·s^{-1})	Area (Fixed)
$Sn_{10}[Ge(SiMe_3)_3]_6$	2.45(2)	1.59(5)	1.05(4)	60
	2.51(2)	0.54(4)	0.79(6)	40

Similar assignments were already done for $Sn_{10}(Hyp)_6$ [19], where the isomer shifts are 2.35(1) and 2.56(1) mm s^{-1}. Consequently, in the case of **1**, the two signals within the spectrum differ by 0.06 mm s^{-1}, while in the case of $Sn_{10}(Hyp)_6$, the difference of 0.21 mm s^{-1} is much larger, being in line with the calculated differences of the charges of the tin atoms inside the cluster. This result shows that the different ligand indeed changes the electronic situation inside the cluster, although the structure remains similar. Additionally, the chemical behavior can be very similar, as seen in the following.

2.2. Li(thf)$_4$Sn$_{10}$[Ge(SiMe$_3$)$_3$]$_5$ **2**

Another metalloid tin cluster that could be achieved by the reaction of the metastable Sn^{I}Cl solution with LiGe(SiMe$_3$)$_3$ · 2.75 THF is Li(thf)$_4$Sn$_{10}$[Ge(SiMe$_3$)$_3$]$_5$ **2**, which is obtained as black crystals from a toluene extract after diverse work-up procedures. The molecular structure of the metalloid cluster anion {Sn$_{10}$[Ge(SiMe$_3$)$_3$]$_5$}$^-$ in **2** is shown in Figure 3, again exhibiting a similar arrangement of the tin atoms in the cluster core as found in the corresponding Hyp derivative [Sn$_{10}$(Hyp)$_5$]$^-$ (Table 3). As well as the comparable structure, the chemical behavior is also similar, as **2** decomposes upon dissolving, hindering further characterization via NMR or electrospray mass spectrometry. However, in the solid state, the compound seems to be stable as the composition of the crystals does not change by time, as shown by energy-dispersive X-ray (EDX) spectroscopy (Supplementary Materials, Figure S11, Table S1).
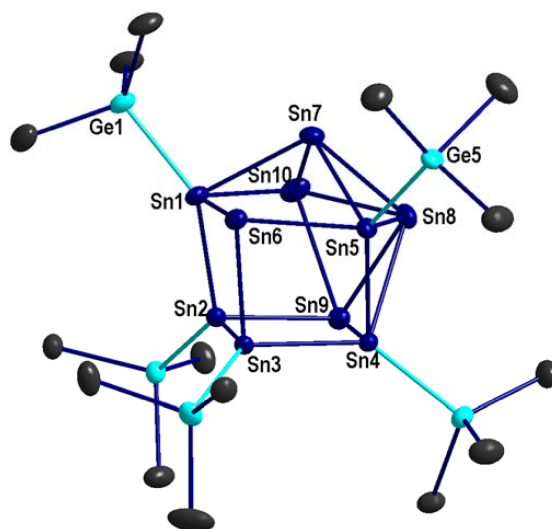
Figure 3. Molecular structure of the anionic metalloid cluster $\{Sn_{10}[Ge(SiMe_3)_3]_5\}^-$, without CH_3 groups (displacement ellipsoids with 50% probability). Selected bond lengths [pm] and angles [°]: Sn1-Sn2: 289.46(2); Sn1-Sn6: 294.95(2); Sn1-Sn7: 295.34(3); Sn1-Sn10: 301.15(3); Sn2-Sn3: 293.69(2); Sn2-Sn9: 287.66(2); Sn3-Sn4: 291.84(2); Sn3-Sn6: 294.31(2); Sn4-Sn5: 292.10(2); Sn4-Sn8: 325.57(3); Sn4-Sn9: 289.73(2); Sn5-Sn6: 294.15(2); Sn5-Sn7: 294.59(3); Sn5-Sn8: 302.91(3); Sn6-Sn7: 329.52(3); Sn7-Sn8: 299.29(3); Sn7-Sn10: 298.05(3); Sn8-Sn9: 303.20(3); Sn8-Sn10: 296.69(3); Sn9-Sn10: 301.88(3); Sn1-Ge1 266.90(3); Sn5-Ge5: 266.62(3); Sn1-Sn2-Sn3: 84.798(6); Sn2-Sn3-Sn4: 83.593(6); Sn2-Sn3-Sn6: 95.120(6); Sn3-Sn4-Sn5: 81.171(6); Sn3-Sn4-Sn8: 113.880(7); Sn4-Sn5-Sn7: 108.572(7); Sn6-Sn5-Sn8: 114.487(8); Sn7-Sn5-Sn8: 60.100(7); Sn7-Sn10-Sn9: 106.442(7); Sn7-Sn10-Sn8: 60.427(7); Ge1-Sn1-Sn6: 115.335(9); Ge5-Sn5-Sn6: 114.513(9).

Table 3. Comparison of the bond lengths in pm of the metalloid clusters $\{Sn_{10}[Ge(SiMe_3)_3]_5\}^-$ and $\{Sn_{10}[Si(SiMe_3)_3]_5\}^-$.

	$\{Sn_{10}[Ge(SiMe_3)_3]_5\}^-$	$\{Sn_{10}[Si(SiMe_3)_3]_5\}^-$
Sn1-Sn2	289.5	288.7
Sn3-Sn4	291.8	293.3
Sn3-Sn6	294.3	294.4
Sn4-Sn5	292.1	292.7
Sn5–Sn8	302.9	302.8
Sn7-Sn10	298.1	297.3
Sn8-Sn9	303.2	302.7
Sn9-Sn10	301.9	302.4

As the behavior of the so-far synthesized metalloid tin clusters, as well as the synthesis, is comparable if Hyp or $Ge(SiMe_3)_3$ is used, we wondered if also the high-yield synthesis of the anionic cluster $[Sn_{10}(Hyp)_4]^{2-}$ with its open ligand shell might be possible, applying $Ge(SiMe_3)_3$ as the substituent as discussed in the following.

2.3. [Li(tmeda)₂]₂Sn₁₀[Ge(SiMe₃)₃]₄ 3

To obtain the anticipated product, we changed the synthetic procedure accordingly. This time, the reaction solution is filtered to remove the metathesis salt, and afterwards, tetramethylethylenediamine (TMEDA) is added as a complexing reagent. In doing so, after a couple of days, black crystals of $[Li(TMEDA)_2]_2Sn_{10}[Ge(SiMe_3)_3]_4$ **3** could be obtained, showing similar crystallographic problems to the Hyp derivative that hinder a proper structure solution. Hence, the black cubic crystals of **3**, obtained by adding TMEDA as a complexing agent, only diffract

well to a 2θ angle of 20°. Recrystallization in the presence of the complexing reagent 12-crown-4 increases the crystal size, but not the crystal quality, and thus the crystal structure could not be solved properly, and only the positions of the Sn, Ge, and Si atoms are refined (Figure 4) [35]. However, the rudimentarily solved crystal structure already shows that the arrangement within the anion $\{Sn_{10}[Ge(SiMe_3)_3]_4\}^{2-}$ in **3** is similar to $[Sn_{10}Hyp_4]^{2-}$ (a comparison of the different tin–tin distances can be found in the Supplementary Materials, Table S2).
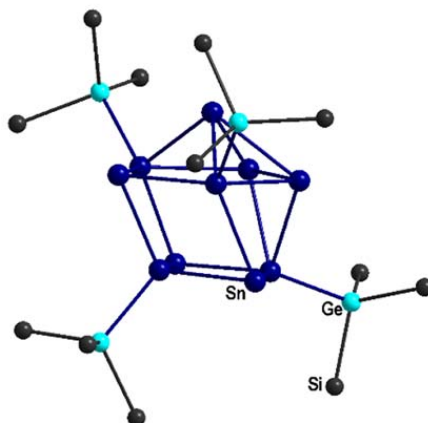

Figure 4. Connectivity map of the cluster core of the anion $\{Sn_{10}[Ge(SiMe_3)_3]_4\}^{2-}$.

Even though **3** is structurally similar to the Hyp derivative $[Sn_{10}(Hyp)_4]^{2-}$, the electronic and chemical characteristics are different. This means that although $\{Sn_{10}[Ge(SiMe_3)_3]_4\}^{2-}$ decomposes like $[Sn_{10}(Hyp)_4]^{2-}$ after dissolving the crystals in THF, this time the decomposition is slower and only after one day at room temperature, a metallic luster on the NMR tube's surface and a black precipitate is observed. The ^{1}H-NMR of freshly dissolved crystals shows a singlet at 0.36 ppm and already some signals of the decomposition products at 0.30 ppm and 0.25 ppm. However, as the decomposition of **3** is slower than the one of the corresponding $[Sn_{10}(Hyp)_4]^{2-}$, it was possible to obtain ^{13}C- and ^{29}Si-NMR data of **3** as well.

To obtain further information about the differences in both $[Sn_{10}R_4]^{2-}$ clusters, an ^{119m}Sn Mössbauer spectrum of **3** is collected. The ^{119m}Sn Mössbauer spectrum of **3** is presented in Figure 5 along with the transmission integral fit. The corresponding fitting parameters for **3** are summarized in Table 4. The cluster shows ten Sn atoms on four different sites (Sn(A), Sn(B), Sn(C), and Sn(D); Figure 6) with different calculated partial charges as obtained from quantum chemical calculations (*vide ultra*). These charges along with the crystallographic information were used to regroup the ten tin atoms in **3**.

Table 4. Fitting parameters for the ^{119m}Sn Mössbauer spectrum of **3** at 6 K; δ = isomer shift, ΔE_Q = electric quadrupole splitting, Γ = experimental line width. Parameters marked with an asterisk (*) were kept fixed during the fitting procedure.

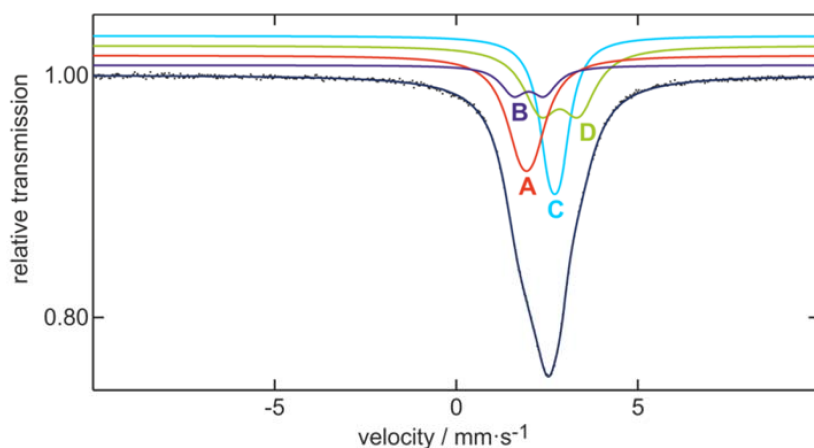| Signal	δ (mm·s⁻¹)	ΔE_Q (mm·s⁻¹)	Γ (mm·s⁻¹)	Ratio (%)
A	1.93(2)	0.36(7)	1.04(6)	30 *
B	2.00(7)	0.8(1)	0.9(1)	10 *
C	2.712(6)	0.31(1)	0.71(1)	30 *
D	2.85(4)	1.05(9)	1.16(2)	30 *

Figure 5. Experimental (data points) and simulated (continuous lines) ^{119m}Sn Mössbauer spectrum of $\{Sn_{10}[Ge(SiMe_3)_3]_4\}^{2-}$ at 6 K. For the fitting parameters, see Table 4.

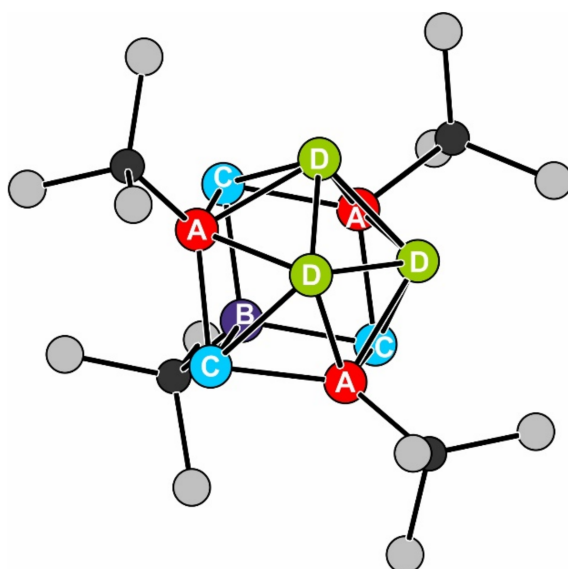**Figure 6.** The cluster core of $\{Sn_{10}[Ge(SiMe_3)_3]_4\}^{2-}$. The different colors of the tin sites correspond to the groups listed in Table 4. For details, see text.

Compared to $[Sn_{10}(Hyp)_4]^{2-}$, showing only one signal for the ten tin atoms at an isomer shift of $\delta = 2.50(1)$ mm s^{-1}, the spectrum of **3** could be well reproduced with four different signals with a fixed area ratio of 1:3:3:3. All four subsignals show isomer shifts between 1.93(2) and 2.85(4) mm s^{-1}, which is in the typical range for Sn(0) species [36] and in very good agreement with recently reported ^{119m}Sn Mössbauer spectroscopic data on similar Sn-cluster compounds such as $[Sn_9(Hyp)_2]^{2-}$ [15], $Sn_{10}[Hyp]_6$ [19], $[Sn_{10}(Hyp)_4]^{2-}$ [17], and $[Sn_{10}(Hyp)_3]^{-}$ [22]. Figure 6 shows the $Sn_{10}(GeSi_3)_4$ core of $\{Sn_{10}[Ge(SiMe_3)_3]_4\}^{2-}$, whereby the four different colors represent the groups of tin atoms which are responsible for the different subsignals.

Signal A shows an isomer shift of 1.93(2) mm s^{-1} and a small quadrupole splitting of 0.36(7) mm s^{-1}. This signal is caused by the red-colored (Figure 6) substituent bound tin atoms Sn(A). The Ge–Sn bond leads to a decreased electron density in comparison to the other Sn atoms. The Sn(A) atoms have four Sn neighbors.

The fourth substituent bound tin atom Sn(B) (dark blue in Figure 6) is just binding to three Sn atoms. This leads to a small difference in the electron density, and results in a slightly increased isomer

shift of 2.00(7) mm s^{-1} (Signal B). The higher quadrupole splitting of 0.8(1) mm s^{-1} is caused by the more asymmetric coordination.

The third signal (C) can be assigned to the light-blue-colored tin atoms of the site Sn(C) with an isomer shift of 2.712(6) mm s^{-1}. The small quadrupole splitting of 0.31(1) mm s^{-1} can be explained by the relatively symmetric coordination by the other Sn atoms in the cluster. The Sn(C) atoms are not bound to a substituent, which leads to a higher electron density in comparison with the tin atoms of the sites Sn(A) and Sn(B).

The green-colored Sn atoms of the site Sn(D) form a tin triangle which has no substituent contacts. The triangle is moved slightly out of the cluster center, which is evident from the Sn bond lengths. Between the Sn atoms from the sites Sn(A) to Sn(C), the Sn–Sn distances are around 290 to 294 pm; bonds to and between the tin atoms of site Sn(D) are longer and about 303 pm. This causes an even higher electron density and thus a higher isomer shift of 2.85(4) mm s^{-1} and a quadrupole splitting of 1.04(6) mm s^{-1} (Signal D). The slightly enhanced line width of signals A and D is caused by the superposition of different tin sites. The small differences cannot be resolved.

3. Materials and Methods

All reactions were carried out under rigorous exclusion of air and moisture using standard Schlenk techniques under nitrogen atmosphere. All solvents were dried and purified by standard procedures.

3.1. LiGe(SiMe₃)₃

LiGe(SiMe$_3$)$_3$ is synthesized by a similar synthetic route to that of the (Hyp) substituent [23]. Therefore, 15.5 mL (24.8 mmol, 1.1 eq) methyllithium solution (1.6 M in Et$_2$O) diluted in 50 mL THF was added dropwise to 8.33 g (22.8 mmol, 1 eq) Ge(SiMe$_3$)$_4$ dissolved in 100 mL THF. The reaction mixture was stirred for 72 h at room temperature and the solvent was removed in vacuo. The remaining white residue was recrystallized in Et$_2$O at −30 °C, whereby pale-yellow crystals of LiGe(SiMe$_3$)$_3$ · 2.75 THF were obtained; yield: 4.68 g (9.4 mmol, 41%). The amount of 2.75 THF is determined via the peak integral ratio in proton NMR compared to that of the SiMe$_3$ groups. ^{1}H-NMR (250 MHz, C$_6$D$_6$): δ = 0.65 (s, 27 H, Si*Me*$_3$), 1.35 (m, 11 H, *CH*$_2$), 3.48 ppm (m, 11 H, O*CH*$_2$). ^{13}C{^{1}H}-NMR (63 MHZ, C$_6$D$_6$): δ = 7.79 (s, Si*Me*$_3$), 25.96 (s, *CH*$_2$), 68.65 ppm (s, O*CH*$_2$). ^{29}Si-NMR (50 MHZ, C$_6$D$_6$): δ = −3.03−−4.71 ppm (m, $^2J_{Si-H}$ = 6.0 Hz, Si*Me*$_3$).

3.2. Sn₁₀(Ge(SiMe₃)₃)₆ (1)

20 mL of a −78 °C cold 0.2 M solution of Sn^{I}Cl in toluene/P*n*Bu$_3$ (volume ratio 10:1; 4 mmol) was added to the −78 °C precooled solid LiGe(SiMe$_3$)$_3$ · 2.75 THF (2.19 g; 4.4 mmol). The reaction mixture was allowed to reach room temperature overnight. The resulting black solution was filtered from the white precipitate and was dried in vacuo. The remaining oil was extracted in pentane, whereby at −30 °C black crystalline blocks of Sn$_{10}$[Ge(SiMe$_3$)$_3$]$_6$ were obtained from the pentane extract; yield: 109 mg (10%). ^{1}H-NMR (250 MHz, C$_6$D$_6$): δ = 0.62 ppm (s, 162H); ^{13}C{^{1}H}-NMR (63 MHz, C$_6$D$_6$) δ = 6.54 ppm (s; SiMe$_3$); ^{29}Si-NMR (50 MHz, C$_6$D$_6$) δ = −0.13−−1.29 ppm (decet, $^2J_{Si-H}$ = 6.5 Hz, Si*Me*$_3$); elemental analysis calc (%) for Sn$_{10}$Ge$_6$Si$_{18}$C$_{64}$H$_{186}$ M$_w$ = 3085.4 g mol^{-1}: C 24.9, H 6.0; found: C 24.7, H 6.0.

3.3. [Li(thf)₄]{Sn₁₀[Ge(SiMe₃)₃]₅} (2)

20 mL of a −78 °C cold 0.2 M solution of Sn^{I}Cl in toluene/P*n*Bu$_3$ (volume ratio 10:1; 4 mmol) was added to the −78 °C precooled solid LiGe(SiMe$_3$)$_3$ · 2.75 THF (2.19 g; 4.4 mmol). The reaction mixture was allowed to reach room temperature overnight to give a black reaction solution. The reaction solution is then filtered from the white precipitate and dried in vacuo to give a black oily residue. The residue was extracted by pentane to give a black pentane extract. On cooling the pentane extract to −30 °C, a black oil precipitated. The solution was filtered and the oil was dissolved in toluene. Storing the black toluene solution at 6 °C gives black hexagonal crystals of Li(thf)$_4$Sn$_{10}$(Ge(SiMe$_3$)$_3$)$_5$;

yield: 48 mg (4%). EDX: calc. (mass %) for $Ge_5Si_{15}Sn_{10}$; M_w = 1971.59 g mol^{-1}: Sn 60.2, Ge 18.4, Si 21.4; found: Sn 56.9; Ge 20.8, Si 22.3. NMR: not possible, due to decomposition of the product in solution.

3.4. [Li(TMEDA)$_2$]$_2${Sn$_{10}$[Ge(SiMe$_3$)$_3$]$_4$} (3)

20 mL of a −78 °C cold 0.2 M solution of Sn^{I}Cl in toluene/PnBu$_3$ (volume ratio 10:1; 4 mmol) was added to the −78 °C precooled solid LiGe(SiMe$_3$)$_3$ · 2.75 THF (2.19 g; 4.4 mmol). The reaction mixture was allowed to reach room temperature overnight to give a black reaction solution. The solution was filtered from the white precipitate and TMEDA (0.2 mL) was added. After 12 h, the solution was filtered from a black crystalline precipitate, which was identified as [Li(tmeda)$_2$]$_2$Sn$_{10}$[Ge(SiMe$_3$)$_3$]$_4$ by single-crystal X-ray diffraction and NMR spectroscopy; yield: 249 mg (22%). These crystals (200 mg, 0.075 mmol) were dissolved in THF at −78 °C and treated with a solution (0.2 mL) of 12-crown-4 in toluene. After a few days at −30 °C, crystals of the metalloid cluster compound [Li(12-crown-4)$_2$]$_2$Sn$_{10}$[Ge(SiMe$_3$)$_3$]$_4$ were obtained.

NMR data of [Li(tmeda)$_2$]$_2$Sn$_{10}$[Ge(SiMe$_3$)$_3$]$_4$: ^{1}H-NMR (250 MHz, C$_6$D$_6$): δ = 0.36 (s, 108 H, Si*Me$_3$*), 2.15 (s, 54 H, tmeda), 2.3 ppm (s, 20 H, tmeda); ^{13}C{^{1}H}-NMR (63MHz, C$_6$D$_6$) δ = 2.61 (s; Si*Me$_3$*), 5.21 (s, Si*Me$_3$*), 46.04 (s, tmeda), 58.76 ppm (s, tmeda); ^{29}Si-NMR (50 MHZ, C$_6$D$_6$) δ = 0.27–1.37 ppm (decet, $^2J_{Si-H}$ = 6.5 Hz, Si*Me$_3$*).

3.5. X-ray Structural Characterization

Crystals were mounted on the diffractometer at 150 K. The data were collected on a Bruker APEX II DUO diffractometer (Bruker AXS Inc., Madison, WI, USA) equipped with an IμS microfocus sealed tube and QUAZAR optics (Icoatec, Geesthacht, Germany) for monochromated MoKα radiation (λ = 0.71073 Å) and equipped with an Oxford Cryosystems cryostat (Oxford Cryosystems Ltd., Oxford, UK). A semiempirical absorption correction was applied using the program SADABS (Bruker AXS Inc., Madison, WI, USA). The structure was solved by Direct Methods and refined against F^2 for all observed reflections. Programs used: SHELXS and SHELXL [37,38] within the Olex2 program package [39]. Both crystallized compounds **1** and **2** showed typical umbrella disorder at some of the Ge(SiMe$_3$)$_3$ substituents and were refined with a disorder model. Additionally, due to heavy disorder of solvent molecules in **1**, not all pentane molecules could be refined properly. Therefore, the SQUEEZE [40] routine was used to identify two voids of 224 Å^3 per unit cell, which contain 41 electrons each, which leads to two more heavy disordered pentane molecules. The supplementary crystallographic data (for ccdc numbers, see below) can be obtained online free of charge at www.ccdc. cam.ac.uk/conts/retrieving.html or from Cambridge Crystallographic Data Centre, 12 Union Road, Cambridge CB21EZ; Fax: (+44)1223-336-033; or deposit@ccdc.cam.ac.uk.

3.5.1. Sn$_{10}$[Ge(SiMe$_3$)$_3$]$_6$

$C_{54}H_{162}Ge_6Si_{18}Sn_{10}$; M_r = 3048.10 g mol^{-1}, crystal dimensions 0.277 × 0.253 × 0.128 mm^3, space group $P2_1/n$, a = 20.7885(5) Å, b = 26.5738(6) Å, c = 23.2212(6) Å, $β$ = 93.2040(10)°, V = 12808.0(5) Å^3, Z = 4, $ρ_{calc.}$ = 1.58 g cm^{-3}, $μ_{Mo}$ = 3.5 mm^{-1}, $2θ_{max}$ = 52.808°, 26,7000 reflections measured, 26,232 independent reflections (R_{int} = 0.0379), absorptions correction: semiempirical (min./max. transmission 0.5818/0.7454), R_1 (I ≥ 2σ) = 0.0281, wR2 (all) = 0.0706, Bruker APEXII diffractometer (MoKα radiation (λ = 0.71073 Å), 150 K). CCDC = 1832611.

3.5.2. [Li(thf)$_4$]{Sn$_{10}$[Ge(SiMe$_3$)$_3$]$_5$}

$C_{61}H_{167}Ge_5Si_{15}Sn_{10}LiO_4$; M_r = 2943.08 g mol^{-1}, crystal dimensions 0.195 × 0.173 × 0.109 mm^3, space group $P2_1/n$, a = 17.2592(3) Å, b = 24.6275(5) Å, c = 30.3649(6) Å, $β$ = 99.2340°, V = 12739.4(4) Å^3, Z = 4, $ρ_{calc.}$ = 1.53 g cm^{-3}, $μ_{Mo}$ = 3.3 mm^{-1}, $2θ_{max}$ = 61.082°, 345748 reflections measured, 38972 independent reflections (R_{int} = 0.0326), absorptions correction: semiempirical (min./max. transmission 0.6391/0.7461), R_1 (I ≥ 2σ) = 0.0276, wR2 (all) = 0.0692, Bruker APEXII diffractometer (MoKα radiation (λ = 0.71073 Å), 150 K). CCDC = 1832610.

3.6. ^{119m}Sn-Mössbauer Spectroscopy

The ^{119m}Sn Mössbauer spectroscopic measurement of $\{Sn_{10}[Ge(SiMe_3)_3]_4\}^{2-}$ and $Sn_{10}[Ge(SiMe_3)_3]_6$ was conducted with a $Ca^{119m}SnO_3$ source in the usual transmission geometry at 6 K. The sample was sealed in a thin-walled quartz container with a sample thickness of about 10 mg Sn cm^{-2}. To reduce the K X-rays emitted by the ^{119m}Sn Mössbauer source, a thin palladium foil (thickness 0.05 mm) was placed in front of the detector. The spectrum was measured over a period of 3 days. Fitting of the spectrum was done with the NORMOS-90 software package [41].

3.7. EDX

EDX analysis was performed by placing the cluster compounds on a graphite carrier into a HITACHI SU8030 scanning electron microscope (Hitachi High Tech Americas Inc. Schaumburg, IL, USA) with BRUKER-EDX (Bruker, Karlsruhe, Germany).

3.8. NMR

^{1}H-, ^{13}C\{^{1}H\}-, and ^{29}Si-INEPT-NMR measurements were done with a Bruker DRX-250 spectrometer (Bruker, Karlsruhe, Germany). All values are given in ppm against the external standard SiMe$_4$.

3.9. Quantum Chemical Calculations

Quantum chemical calculations were carried out with the RI-DFT version [27] of the Turbomole program package (Turbomole GmbH, Karlsruhe, Germany) [24] and the TmoleX graphical user interface (Cosmologic GmbH, Leverkusen, Germany) [33] by employing the BP86 functional [25,26]. The basis sets were of SVP quality [28]. All model compounds are calculated as being structurally optimized. Partial charges of all atoms are calculated via an Ahlrichs–Heinzmann population analysis [29–32] (see Supplementary Materials for further details).

4. Conclusions

The disproportionation reaction of metastable Sn(I) halides proved to be a useful synthetic route to metalloid tin clusters, where the new Ge(SiMe$_3$)$_3$ ligand is used to obtain the metalloid cluster compounds $Sn_{10}[Ge(SiMe_3)_3]_6$ **1**, $[Li(thf)_4]\{Sn_{10}[Ge(SiMe_3)_3]_5\}$ **2**, and $[Li(TMEDA)_2]_2\{Sn_{10}[Ge(SiMe_3)_3]_4\}$ **3**. The ten tin atoms within these clusters are arranged in the form of a distorted centaur polyhedron being isostructural to the corresponding Hyp derivatives $Sn_{10}(Hyp)_6$, $[Sn_{10}(Hyp)_5]^-$, and $[Sn_{10}(Hyp)_4]^{2-}$. However, **1**, **2**, and **3** show electronic differences to their Hyp derivatives, as revealed by ^{119m}Sn Mössbauer spectroscopy, and also show slightly different stabilities. The now-available metalloid tin clusters with different substituents can be used in further investigations to reveal the influence of the substituent on the reactivity of a metalloid tin cluster, where especially the metalloid tin cluster $\{Sn_{10}[Ge(SiMe_3)_3]_4\}^{2-}$ is of central importance due to its open ligand shell and moderate yield synthesis (22%). Here, deeper insight into the formation mechanism of the recently obtained intermetalloid cluster $[Au_3Sn_{18}(Hyp)_8]^-$ might also be possible as now reagents with different substituents are available, which is a part of ongoing research in our laboratory.

Supplementary Materials: Supplementary materials are available online. 1: results of quantum chemical calculations; 2: NMR spectra, Figures S5–S10; 3: Results of EDX measurements. 4. Bond length comparison of $\{Sn_{10}[Ge(SiMe_3)_3]_4\}^{2-}$ and $[Sn_{10}(Hyp)_4]^{2-}$.

Author Contributions: M.B. and A.S. conceived and designed the experiments, M.B. performed the experiments, T.B. and R.P. conducted and analyzed the Mössbauer data, and C.S. performed the X-ray crystal structure analysis and the quantum chemical calculations. M.B. and A.S. wrote the paper.

References and Notes

1. Goesmann, H.; Feldmann, C. Nanoparticulate Functional Materials. *Angew. Chem. Int. Ed.* **2010**, *49*, 1362–1397. [CrossRef] [PubMed]

2. Schnepf, A. Structure and Bonding. In *Clusters—Contemporary Insight in Structure and Bonding*; Dehnen, S., Ed.; Springer: Cham, Switzerland, 2017; Volume 174, pp. 135–200.

3. Schnepf, A. Metalloid group 14 cluster compounds: An introduction and perspectives to this novel group of cluster compounds. *Chem. Soc. Rev.* **2007**, *36*, 745–758. [CrossRef] [PubMed]

4. Schnöckel, H. Structures and Properties of Metalloid Al and Ga Clusters Open Our Eyes to the Diversity and Complexity of Fundamental Chemical and Physical Processes during Formation and Dissolution of Metals. *Chem. Rev.* **2010**, *110*, 4125–4163. [CrossRef] [PubMed]

5. Jin, R. Quantum sized, thiolate-protected gold nanoclusters. *Nanoscale* **2010**, *2*, 343–362. [CrossRef] [PubMed]

6. Schrenk, C.; Schnepf, A. Metalloid Sn clusters: Properties and the novel synthesis via a disproportionation reaction of a monohalide. *Rev. Inorg. Chem.* **2014**, *36*, 93–118. [CrossRef]

7. Binder, M.; Schrenk, C.; Schnepf, A. The Synthesis of $[Sn_{10}(SiMe_3)_3)_4]^{2-}$ using a Metastable Sn(I) Halide Solution Synthesized via Co-condensation Technique. *J. Vis. Exp.* **2016**, *117*, e54498.

8. Another fruitful route for the synthesis of metalloid tin clusters applies the reductive coupling of respective starting compounds giving metalloid tin clusters with up 17 tin atoms in the cluster core [9–14].

9. Eichler, B.E.; Power, P.P. Synthesis and Characterization of $[Sn_8(2,6-Mes_2C_6H_3)_4]$ (Mes = $2,4,6-Me_3C_6H_2$): A Main Group Metal Cluster with a Unique Structure. *Angew. Chem. Int. Ed.* **2001**, *40*, 796–797. [CrossRef]

10. Richardson, A.F.; Eichler, B.E.; Brynda, M.; Olmstead, M.M.; Power, P.P. Metal-Rich, Neutral and Cationic Organotin Cluster. *Angew. Chem. Int. Ed.* **2005**, *44*, 2546–2549. [CrossRef] [PubMed]

11. Brynda, M.; Herber, R.; Hitchcock, P.B.; Lappert, M.F.; Nowik, I.; Power, P.P.; Protchenko, A.V.; Ruzicka, A.; Steiner, J. Higher-Nuclearity Group 14 Metalloid Clusters: $[Sn_9\{Sn(NRR')\}_6]$. *Angew. Chem. Int. Ed.* **2006**, *45*, 4333–4337. [CrossRef] [PubMed]

12. Rivard, E.; Steiner, J.; Fettinger, J.C.; Giuliani, J.R.; Augustine, M.P.; Power, P.P. Convergent syntheses of $[Sn_7\{C_6H_3-2,6-(C_6H_3-2,6-iPr_2)_2\}_2]$: A cluster with a rare pentagonal bipyramidal motif. *Chem. Commun.* **2007**, 4919–4921. [CrossRef]

13. Prabusankar, G.; Kempter, A.; Gemel, C.; Schröter, M.-K.; Fischer, R.A. $[Sn_{17}\{GaCl(ddp)\}_4]$: A High-Nuclearity Metalloid Tin cluster Trapped by Electrophilic Gallium Ligands. *Angew. Chem. Int. Ed.* **2008**, *47*, 7234–7237. [CrossRef] [PubMed]

14. Wiederkehr, J.; Wölper, C.; Schulz, S. Synthesis and solid state structure of a metalloid tin cluster $[Sn_{10}(trip_8)]$. *Chem. Commun.* **2016**, *52*, 12282–12285. [CrossRef] [PubMed]

15. Schrenk, C.; Winter, F.; Pöttgen, R.; Schnepf, A. $\{Sn_9[Si(SiMe_3)_3]_2\}^{2-}$: A Metalloid Tin Cluster Compound with a Sn_9 Core of Oxidation State Zero. *Inorg. Chem.* **2012**, *51*, 8583–8588. [CrossRef] [PubMed]

16. Schrenk, C.; Neumaier, M.; Schnepf, A. $\{Sn_9[Si(SiMe_3)_3]_3\}^-$ and $\{Sn_8Si[Si(SiMe_3)_3]_3\}^-$: Variations of the E9 Cage of Metalloid Group 14 Clusters. *Inorg. Chem.* **2012**, *51*, 3989–3995. [CrossRef] [PubMed]

17. Schrenk, C.; Winter, F.; Pöttgen, R.; Schnepf, A. $\{Sn_{10}[Si(SiMe_3)_3]_4\}^{2-}$: A Highly Reactive Metalloid Tin Cluster with an Open Ligand Shell. *Chem. Eur. J.* **2015**, *21*, 2992–2997. [CrossRef] [PubMed]

18. Schrenk, C.; Helmlinger, J.; Schnepf, A. $\{Sn_{10}[Si(SiMe_3)_3]_5\}^-$: An Anionic Metalloid Tin Cluster from an Isolable SnI Halide Solution. *Z. Anorg. Allg. Chem.* **2012**, *638*, 589–593. [CrossRef]

19. Schrenk, C.; Schellenberg, I.; Pöttgen, R.; Schnepf, A. The formation of a metalloid $Sn_{10}[Si(SiMe_3)_3]_6$ cluster compound and its relation to the α↔β tin phase transition. *Dalton Trans.* **2010**, *39*, 1872–1876. [CrossRef] [PubMed]

20. Kotsch, M.; Gienger, C.; Schrenk, C.; Schnepf, A. The Sterically Demanding Thiosilyl Group $SSi(SiMe_3)_3$ as a Ligand in Transition Metal Chemistry. *Z. Anorg. Allg. Chem.* **2016**, *642*, 670–675. [CrossRef]

21. Binder, M.; Schrenk, C.; Block, T.; Pöttgen, R.; Schnepf, A. [Hyp-Au-Sn_9(Hyp)$_3$-Au-Sn_9(Hyp)$_3$-Au-Hyp]$^-$: The longest intermetalloid chain compound of tin. *Chem. Commun.* **2017**, *53*, 11314–11317. [CrossRef] [PubMed]

22. Schrenk, C.; Gerke, B.; Pöttgen, R.; Clayborne, A.; Schnepf, A. Reactions with a Metalloid Tin Cluster {Sn$_{10}$[Si(SiMe$_3$)$_3$]$_4$}$^{2-}$: Ligand Elimination versus Coordination Chemistry. *Chem. Eur. J.* **2015**, *21*, 8222–8228. [CrossRef] [PubMed]

23. Gilman, H.; Smith, C.L. Tetrakis(trimethylsilyl)silane. *J. Organomet. Chem.* **1967**, *8*, 245–253. [CrossRef]

24. Treutler, O.; Ahlrichs, R. Efficient molecular numerical integration schemes. *J. Chem. Phys.* **1995**, *102*, 346–354. [CrossRef]

25. Perdew, J.P. Density-functional approximation for the correlation energy of inhomogeneous electron gas. *Phys. Rev. B* **1986**, *33*, 8822–8884. [CrossRef]

26. Becke, A.D. Density-functional exchange-energy approximation with correct asymptotic behavior. *Phys. Rev. A* **1988**, *38*, 3098–3100. [CrossRef]

27. Eichkorn, K.; Treutler, O.; Öhm, H.; Häser, M.; Ahlrichs, R. Auxiliary basis sets to approximate Coulomb potentials. *Chem. Phys. Lett.* **1995**, *240*, 283–290. [CrossRef]

28. Schäfer, A.; Horn, H.; Ahlrichs, R. Fully optimize contracted Gaussian basis sets for atoms Li to Kr. *J. Chem. Phys.* **1992**, *97*, 2571–2577. [CrossRef]

29. Davidson, E.R. Electronic population analysis of molecular Wavefunctions. *J. Chem. Phys.* **1967**, *46*, 3320–3324. [CrossRef]

30. Roby, K.R. Quantum theory of chemical valence concepts. *Mol. Phys.* **1974**, *27*, 81–104. [CrossRef]

31. Heinzmann, R.; Ahlrichs, R. Population analysis based on occupation numbers of modified atomic orbitals (MAOs). *Theor. Chim. Acta* **1976**, *42*, 33–45. [CrossRef]

32. Erhardt, C.; Ahlrichs, R. Population analysis based on occupation numbers II. Relationship between shared electron numbers and bond energies and characterization of hypervalent contributions. *Theor. Chim. Acta* **1985**, *68*, 231–245. [CrossRef]

33. Steffen, C.; Thomas, K.; Huniar, U.; Hellweg, A.; Rubner, O.; Schroer, A. TmoleX-A graphical user interface for TURBOMOLE. *J. Comput. Chem.* **2010**, *31*, 2967–2970. [CrossRef] [PubMed]

34. The Shared Electron Numbers (SENs) for Bonds are Reliable Measure of the Covalent Bonding Strength. For Example, the Sen for the Sn-Sn Single Bond in (SiH$_3$)$_3$Sn-Sn(SiH$_3$)$_3$ is 1.11; Whereas the SEN for a Double Bond in (SiH$_3$)$_2$Sn = Sn(SiH$_3$)$_2$ is 1.48.

35. The molecular structure of [Li(tmeda)$_2$]$_2$Sn$_{10}$[Ge(SiMe$_3$)$_3$]$_4$ was rudimentarily solved in the orthorhombic crystal system with a = 16.2915(15), b = 30.669(3), c = 33.450(3) Å in space group *Pbcm* with half a molecule in the asymmetric unit.

36. Shenoy, G.F.; Wagner, F.E. *Mößbauer Isomer Shifts*; North-Holland Publishing Company: Amsterdam, The Netherland, 1978.

37. Sheldrick, G.M. A short history of SHELX. *Acta Crystallogr.* **2008**, *A64*, 112–122. [CrossRef] [PubMed]

38. Sheldrick, G.M. Crystal structure refinement with SHELX. *Acta Crystallogr.* **2015**, *C71*, 3–8.

39. Dolomanov, O.V.; Bourhis, L.J.; Gildea, R.J.; Howard, J.A.K.; Puschmann, H. OLEX2: A complete structure solution, refinement and analysis program. *J. Appl. Crystallogr.* **2009**, *42*, 339–341. [CrossRef]

40. Spek, A.L. Single-crystal structure validation with the program PLATON. *J. Appl. Cryst.* **2003**, *36*, 7–13. [CrossRef]

41. Brand, R.A. *Normos Mössbauer Fitting Program*; University of Duisburg: Duisburg, Germany, 2002.

Sample Availability: Samples of the compounds are available from the authors.